Supplementary material for 'Comparison of particle number size distribution trends in ground measurements and climate models' by Leinonen et al.

S1 Seasonality, SeasC and NIQR

Seasonality of measured and modelled N were compared using SeasC for maximum seasonal variation and NIQR for average seasonal variation. In this seasonal comparison, we have concentrated on Aitken and accumulation modes. The results for the nucleation mode are shown in Fig. S11 for maximum variation and in Fig. S14 for average variation. In Figures S12 and S13, maximum variations are shown for Aitken and accumulation mode, respectively. The figures also indicate during which season the minimum and maximum values usually occur.

The maximum variation of medians of measured data values were mostly insensitive to the representation of the data, especially for the accumulation mode, although interquartile ranges did show some variation with varying measurement data representation. Notable exceptions to this general statement were the Aitken mode SeasC values for Zeppelin, K-Puszta, and San Pietro Capofiume. The strong dependence of the Aitken mode SeasC on data representation at Zeppelin is most likely due to the very clean conditions there, which easily leads to large variations in relative changes. At K-Puszta and San Pietro Capofiume, the results from measurement representations appeared to be very sensitive to the assumed upper bound of the Aitken mode, which is 50 nm for the sectional representation and 100 nm for the modal representation. This could result in a shift of particle number between Aitken and accumulation modes and hence could affect the computed SeasC value, especially if the effect was different for different seasons. This becomes apparent when comparing Figs. S12 and S13, where for these two sites the sectional representation had a larger Aitken mode SeasC and a smaller accumulation mode SeasC. The season during which the minimum and maximum values in N occur were also mostly independent of data representation, but in some cases shifted to an earlier or later season.

For maximum variation (SeasC) in measured data, there was a clear difference between remote and more polluted sites, with seasonal variations in Ns being higher in remote sites. Remote sites had generally larger maximum variation due to the more dominating effect of naturally emitted (organic) particles and particle precursors during summer, which was affecting especially the Aitken mode maximum N and, hence increasing maximum variation. For measured maximum variation, three sites, Zeppelin (polar), Pallas (remote), and Värriö (remote) had the highest maximum variation, meaning that N in summer could be 3-10 times higher than concentrations in winter. For urban and other polluted sites, seasonal variation was much smaller, having maximum variation values of less than 2. Results for measured maximum variation with respect to site classes were consistent with findings of Rose et al. (2021), who presented SeasC results for total Ns measured in 62 sites globally in 2016 or 2017.

ECHAM-SALSA, NorESM1.2, and UKESM1 had larger maximum variation for polar and remote sites than for urban sites, which was also observed in measurements. However, sometimes the maximum variation was overestimated. ECHAM-SALSA and NorESM1.2 especially seemed to overestimate the Aitken mode maximum variation in many of the sites investigated in this study. For northern sites, Pallas, Värriö, and Zeppelin, higher maximum variation in models was not the only difference, but also the seasonal cycle in these two models was similar to the measured, but different compared to the other three models, as seen for example for Aitken mode in Fig. 14. In addition, compared to the observed

modes in Hyytiälä, Melpitz, K-Puszta, Vavihill, Puijo, and Helsinki, NorESM1.2 and ECHAM-SALSA had lower Ns especially during winter, and this results in higher annual variation.

In Figures S15 and S16, measured average seasonal variation in Aitken and accumulation mode N was investigated with NIQR. NIQR had similar patterns as SeasC. This was expected, as both quantities measure seasonal variation, with SeasC focusing more on extreme values. For Aitken mode, the largest average variations were seen in remote sites Zeppelin, Pallas, and Värriö. For accumulation mode, the differences were smaller, remote sites having the largest values, which were smaller than for Aitken mode. In addition, models seemed to mostly capture average seasonal variation similarly as they captured maximum variation in Aitken and accumulation mode.

In general, models captured average seasonal variation (NIQR) slightly better than maximum variations (SeasC). Variability in the interquartile range was, therefore, better accounted for than the seasonal extremes, which were resulting in higher modelled maximum variation than observations. The reason for higher maximum variation is diverse: for Aitken mode, it is usually due to underestimated lowest interquartile range and especially too small concentrations observed during winter months, whereas for accumulation mode, higher modelled concentrations during summer were usually causing too high maximum variation in models. However, in the big picture, the seasonality variables (NIQR and SeasC) got larger values in remote areas and smaller values in more polluted areas, which was seen in the models even though the magnitude of the seasonality was overestimated or underestimated.

For measured seasonal extremes in the Aitken mode, almost all sites had their minimum concentrations in winter or autumn. Only San Pietro Capofiume had its minimum in Spring. At the other sites, maxima in Aitken mode were either in summer or spring. The seasonal pattern for Aitken mode concentrations was not similar in models compared to measurements, where NorESM1.2 seemed to capture seasonal extremes best, except the magnitude of extremes, which was sometimes overestimated. Aitken mode minimum was more often captured by the models than maximum.

For Accumulation mode, measurements did not show clear differences in average seasonal variation and maximum variation of number concentration between remote and other sites, despite measured maximum variation had on average been slightly larger for remote sites. However, maximum variation of accumulation mode N was smaller than maximum variation of Aitken mode in remote sites. Especially NorESM1.2 and also ECHAM-SALSA seemed to overestimate the maximum variation of the Accumulation mode N in most of the sites. These overestimates were in almost all cases due to higher modelled Ns in summer compared to what has been observed.

For seasonal extremes in the accumulation mode, most of the sites had their (observational) minimum concentration either in winter or autumn and maximum in spring or summer. Exceptions were San Pietro Capofiume where the minimum was during spring and maximum in winter, Mace Head where minimum was during summer and maximum during spring, and K-Puszta where the minimum was during summer and maximum in winter. Summer maxima were mostly captured by the models, and in general better than for Aitken mode. For the accumulation mode, the season of maximum number concentration was better captured by the models than the minimum.

The annual cycles of Ns varied between models, modes, and sites. When calculating the total number of seasonal extremes captured by the models, ECHAM-SALSA captured most of the seasonal extremes in nucleation, Aitken, and accumulation mode for all sites (34 correct seasons/78 = 6 extremes * 13 sites), followed by NorESM1.2 (33), ECHAM-SALSA (30), UKESM (30) and EC-Earth (22) when model extremes were compared to mode fitting results. Results were varying between different modes, ECHAM-M7 and ECHAM-SALSA had best captured the nucleation mode extremes. NorESM1.2 was best for Aitken mode and UKESM1 showed the best results for accumulation mode.

S2 Additional figures
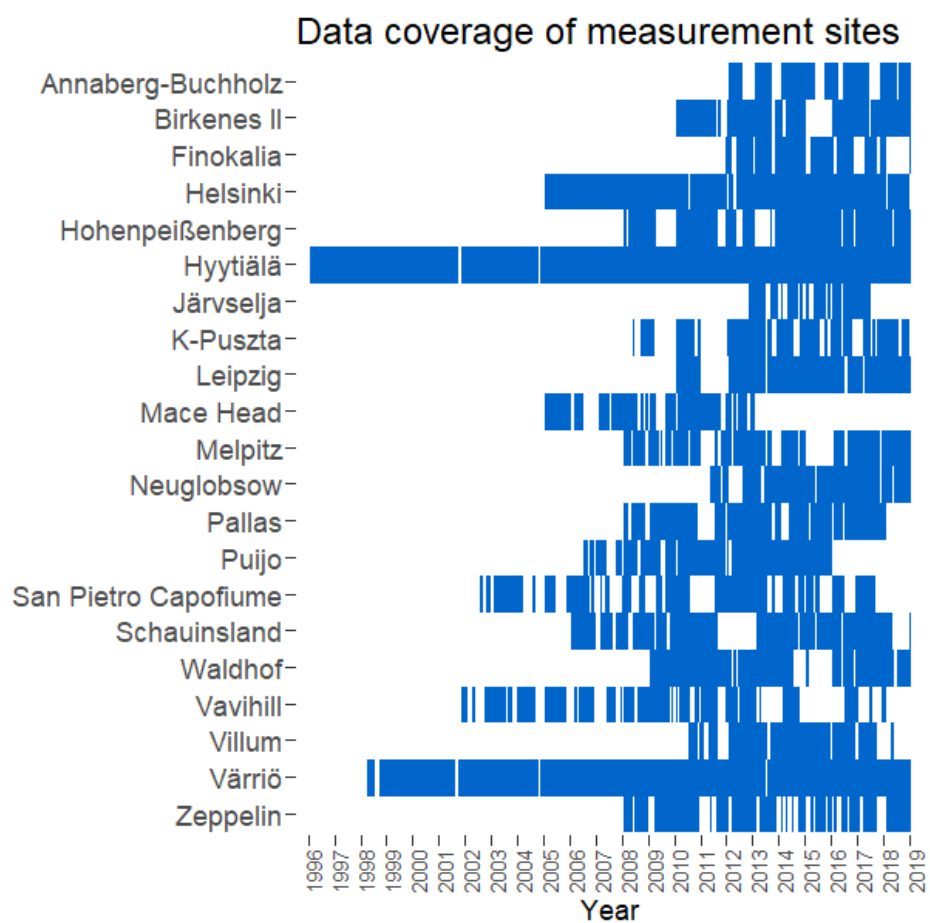
Figure S1 Data coverage of measurement sites. Blue represents the periods where daily averaged data have been calculated, i.e., there is at least 5 measurement points/day. The data coverage of the sites is between 59.6 and 98.4% of the days in the measured period.
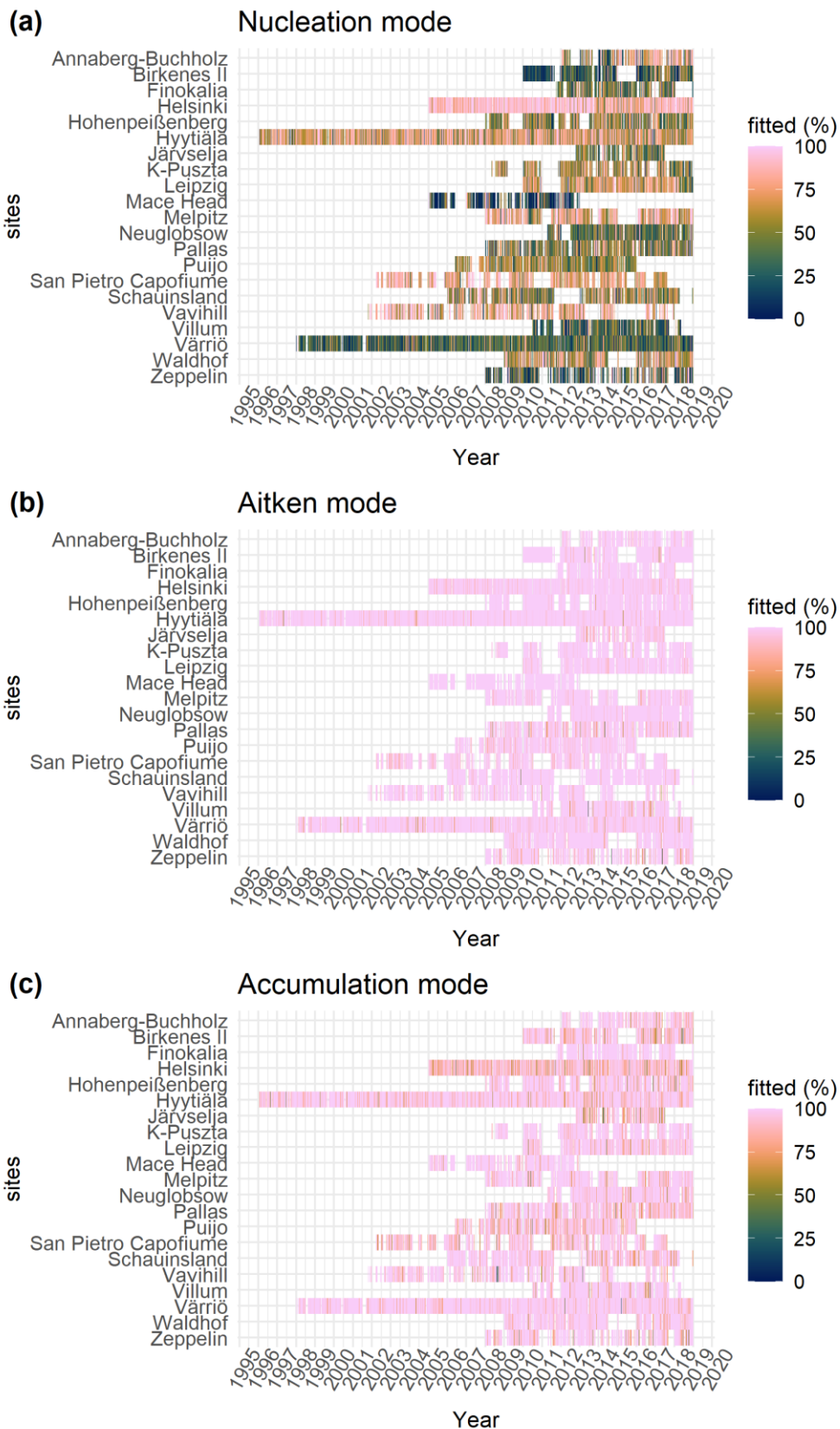
Figure S2 Percentages of fitted nucleation (a), Aitken (b), and accumulation (c) modes at each day and at different sites during the whole measurement time series.
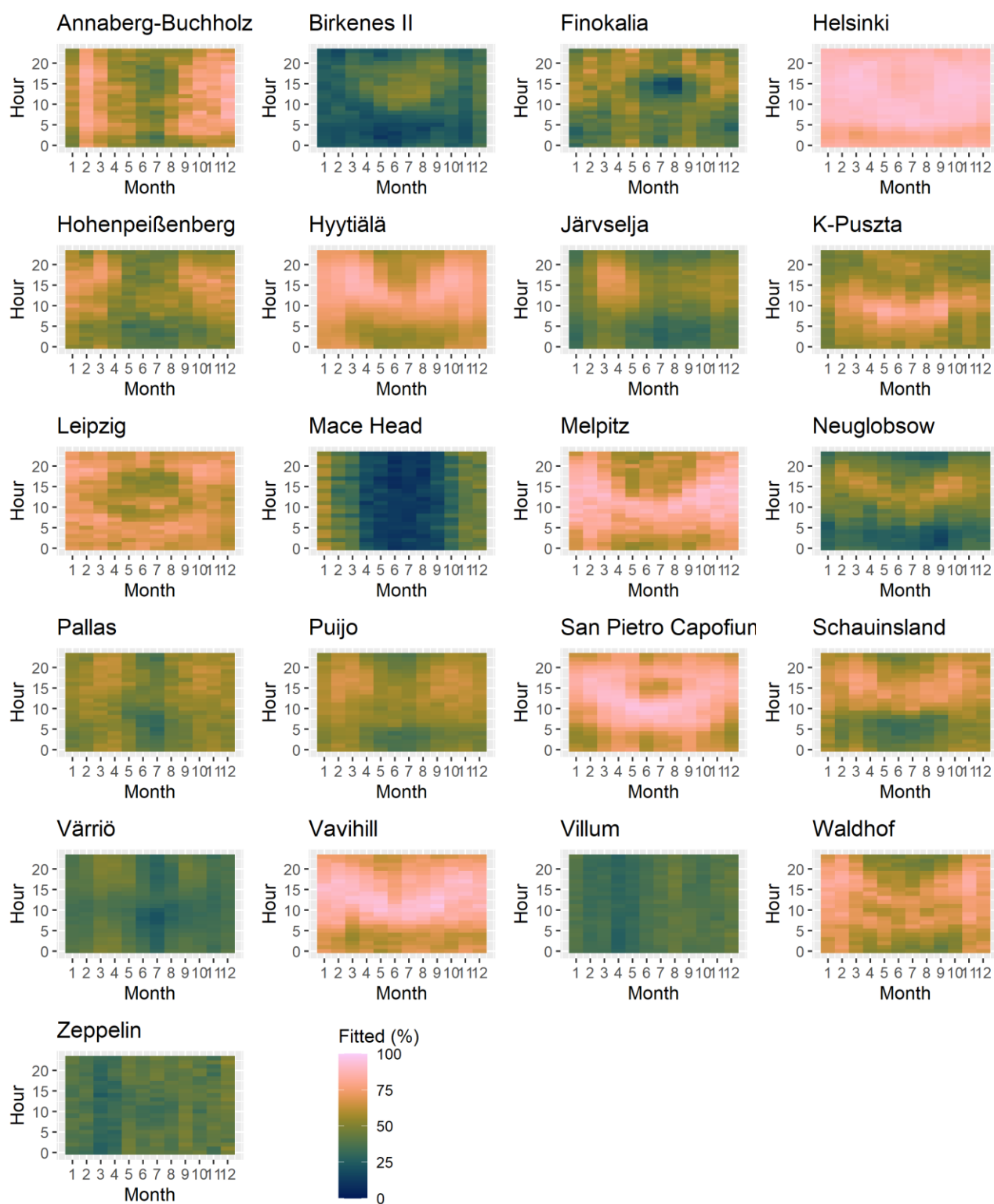
Figure S3 Mean percentages of fitted nucleation modes at each hour and month at different sites during the whole measurement time series.
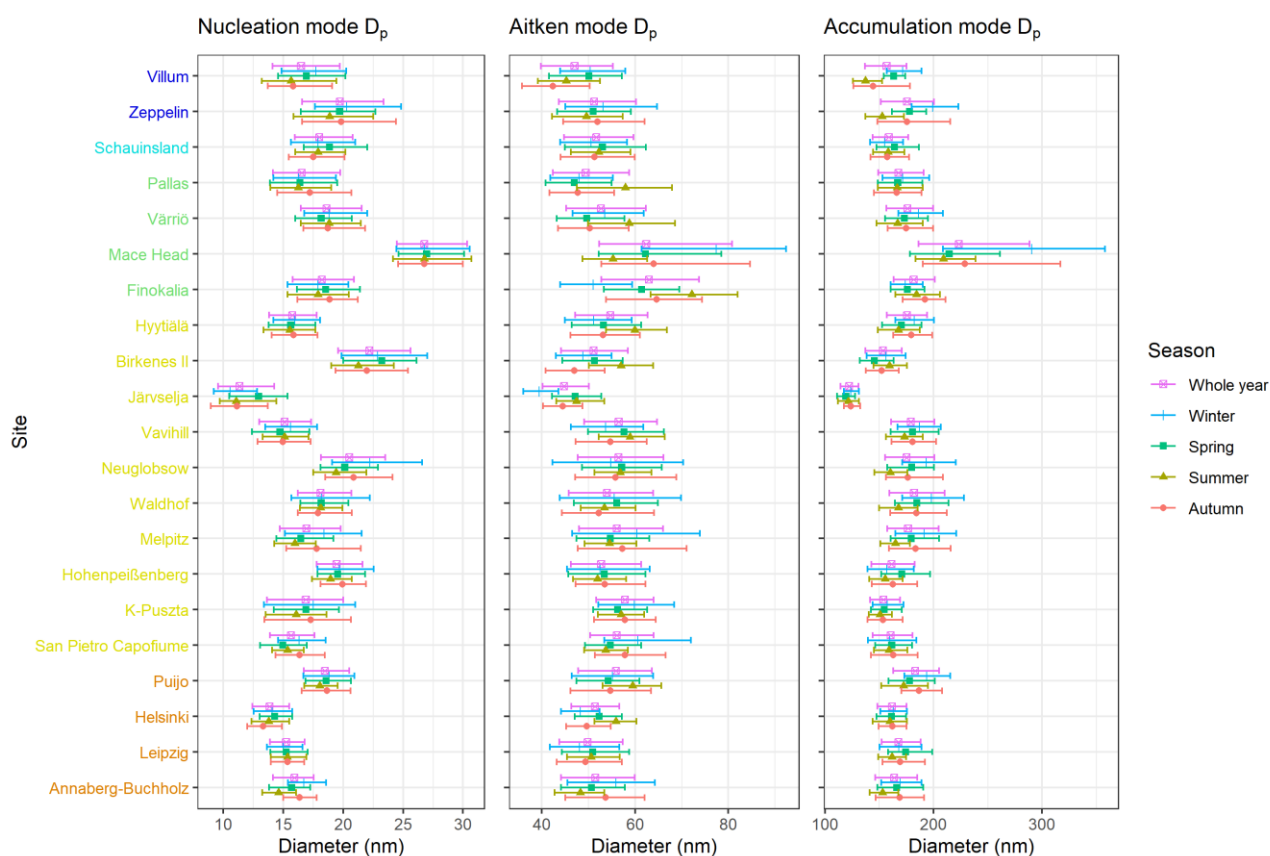
Figure S4 **Summary of geometric mean diameter D_p for measurement sites and different seasons. Medians (dots) and interquartile ranges (25% and 75%, whiskers) for different mode parameters in fitted modes.**
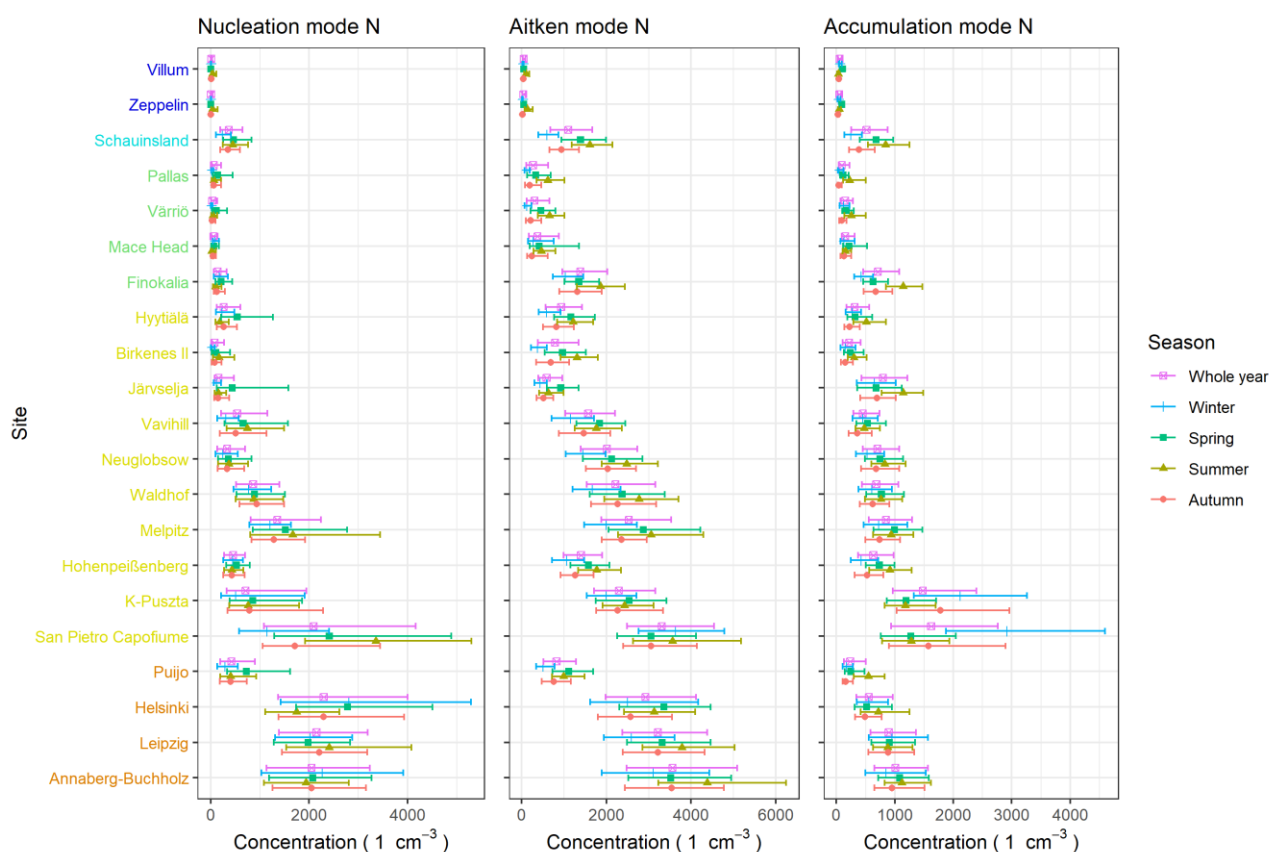
Figure S5 Summary of number concentration diameter (N) for measurement sites and different seasons. Medians (dots) and interquartile ranges (25% and 75%, whiskers) for different mode parameters in fitted modes.
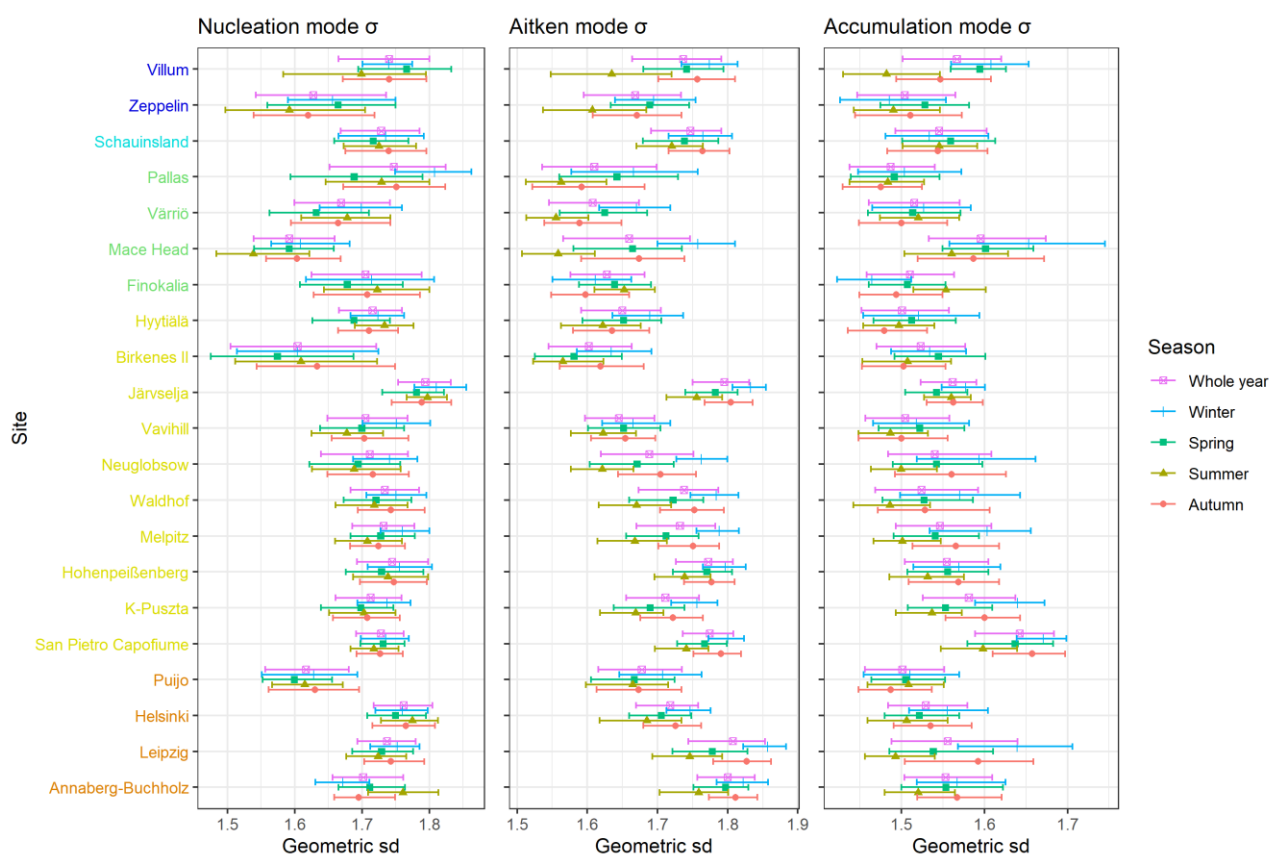
Figure S6 Summary of geometric standard deviation σ for measurement sites and different seasons. Medians (dots) and interquartile ranges (25% and 75%, whiskers) for different mode parameters in fitted modes.
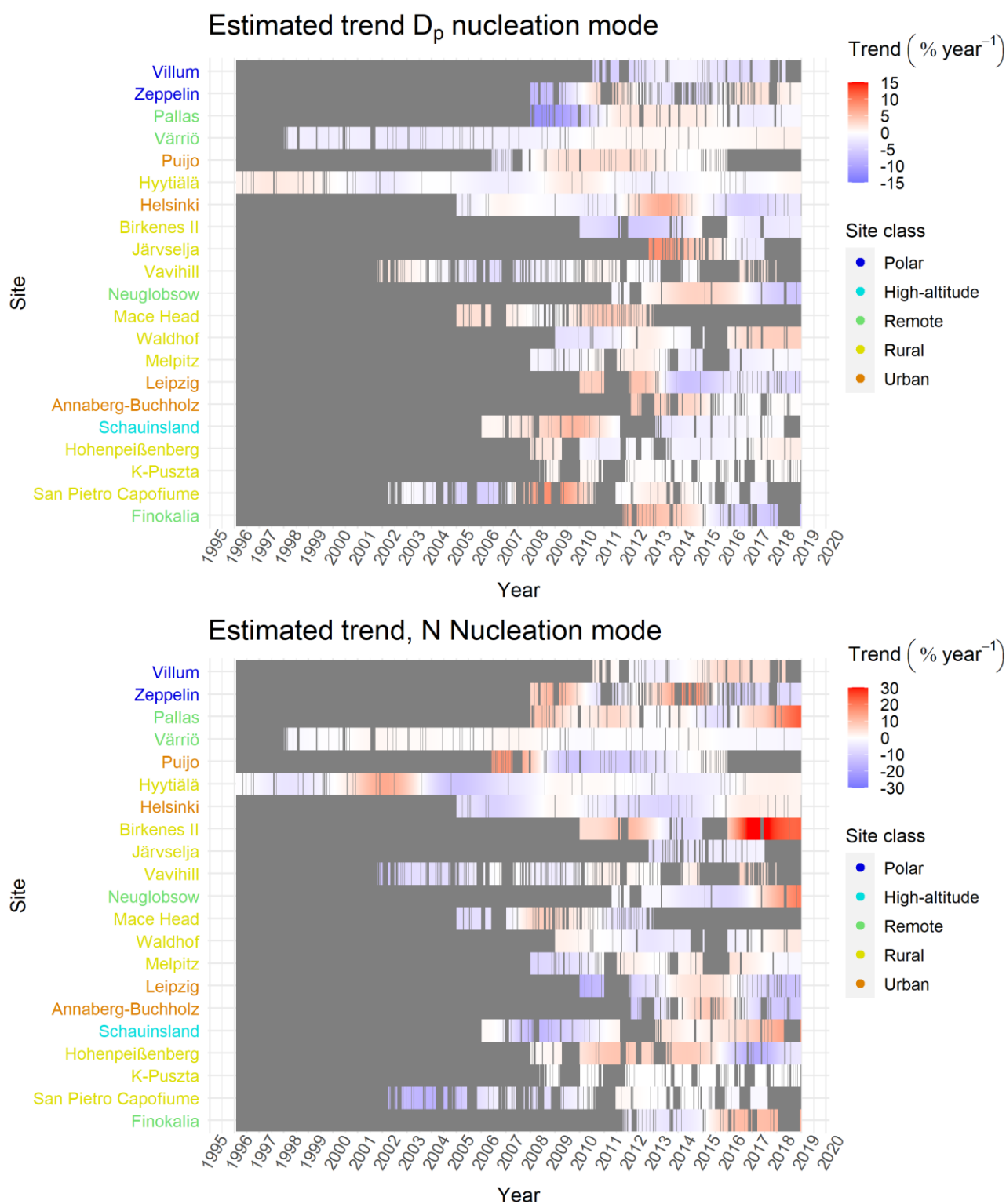
Figure S7 Estimated trends for nucleation mode D_p and N at measurement sites. Trend has been calculated by DLM, see section 2.3.1 for details. The overall trend presented in the figure is comparable with the long-term trend estimates given in section 3.1. To get a DLM trend for one year, the one-day trend given by the model was multiplied by the number of days in a year (365 used for all years) and divided by the mean of the variable over the first observed year. For example, if the trend is showing an increase of 10% / year it means that if the short-term increase would continue for a year, the concentration would be increased by 10% during the year compared to the first year mean.
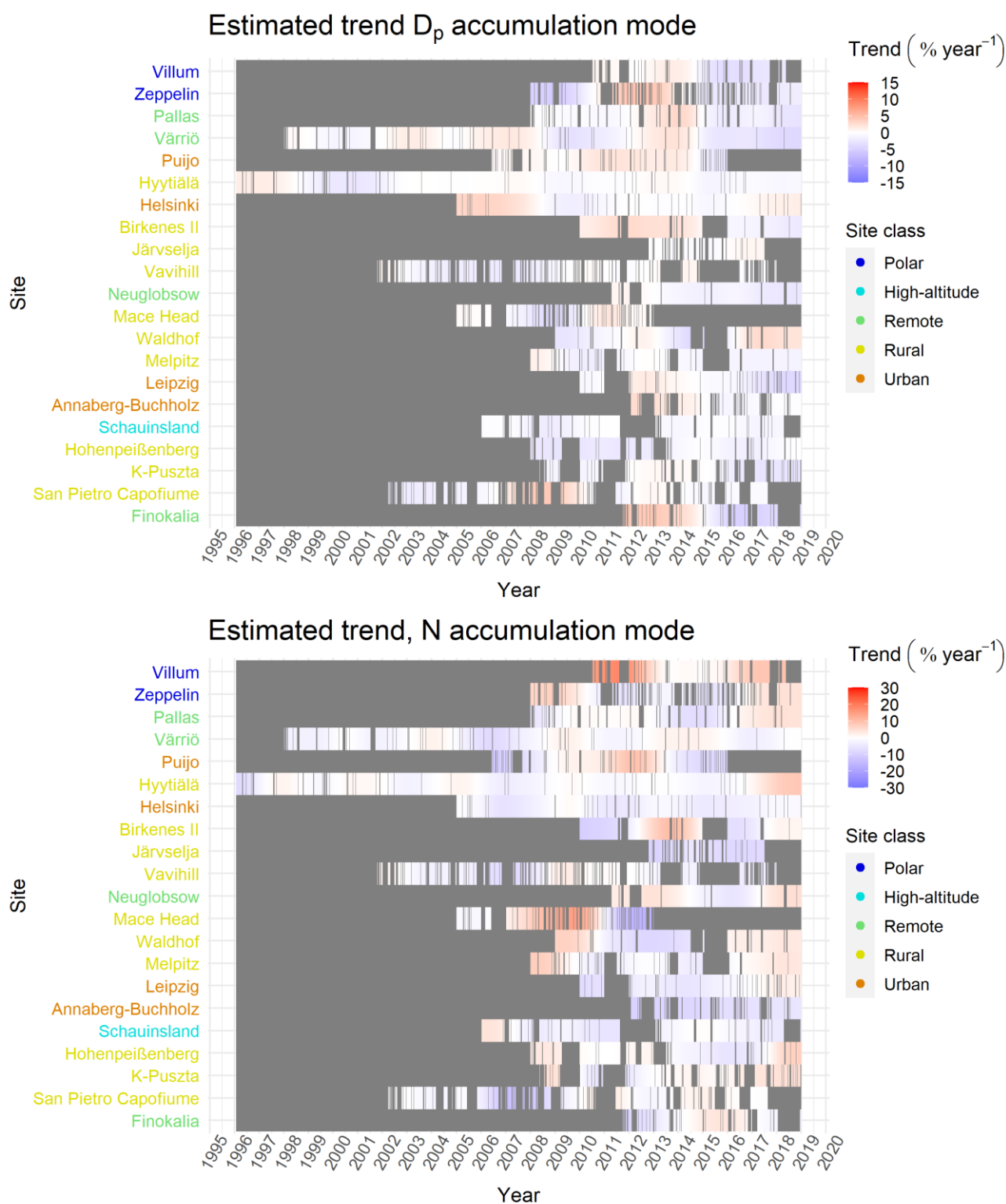
Figure S8 Estimated trends for accumulation mode D_p and N at measurement sites. Trend has been calculated by DLM, see section 2.3.1 for details. The overall trend presented in the figure is comparable with the long-term trend estimates given in section 3.1. To get a DLM trend for one year, the one-day trend given by the model was multiplied by the number of days in a year (365 used for all years) and divided by the mean of the variable over the first observed year. For example, if the trend is showing an increase of 10% / year it means that if the short-term increase would continue for a year, the concentration would be increased by 10% during the year compared to the first year mean.
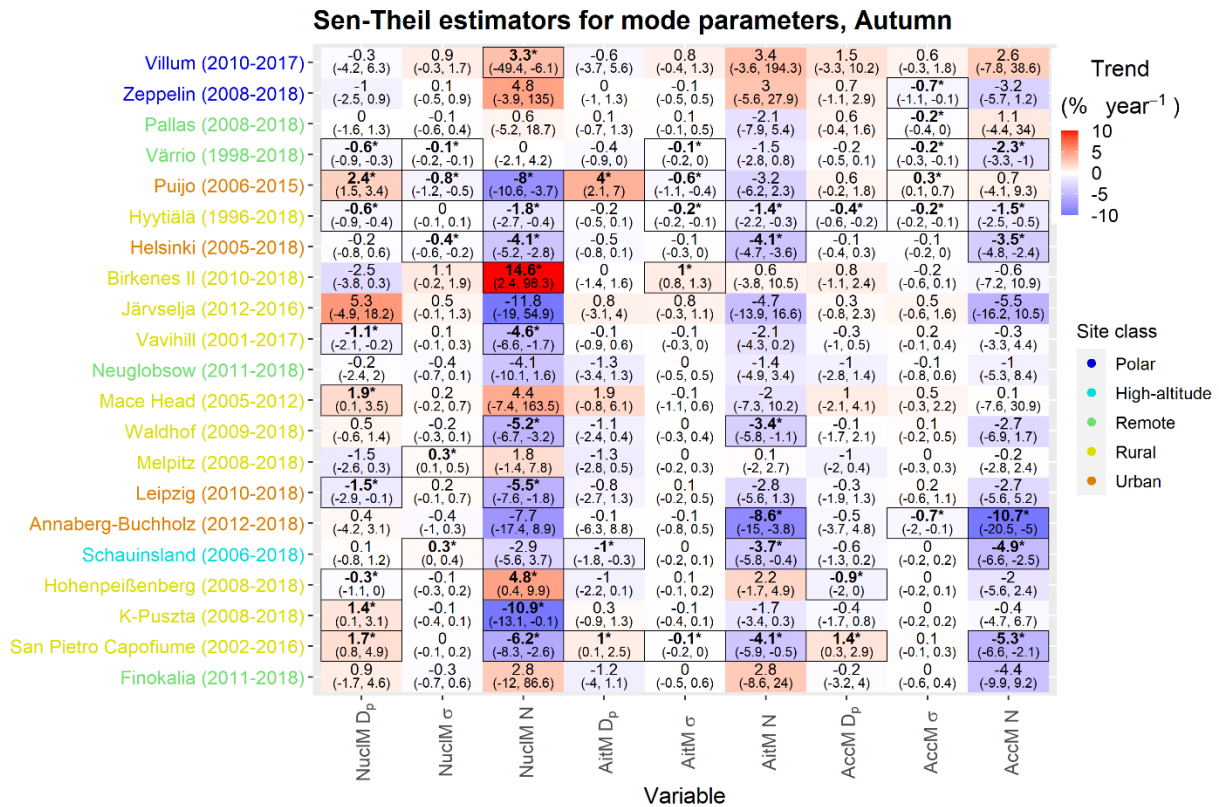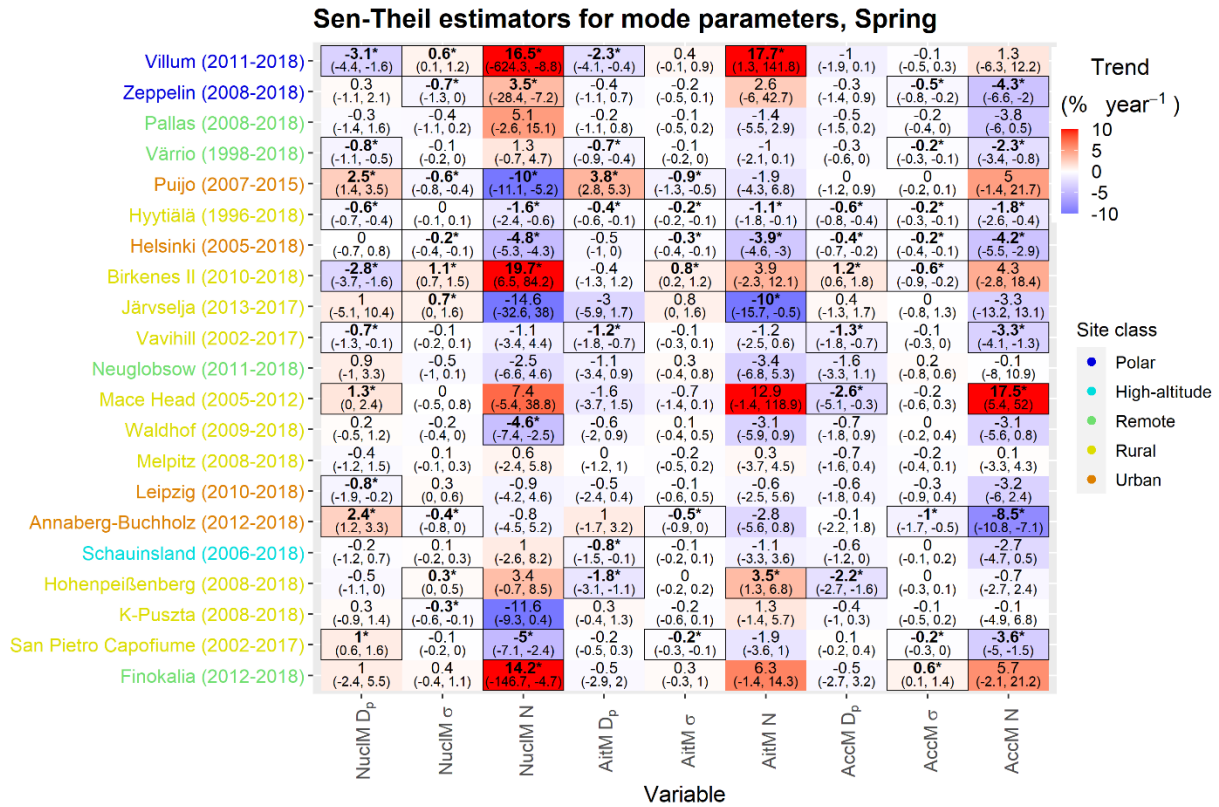
Figure S9 Seasonal long-term trend estimates for all mode parameters (mean geometric diameter D_p, geometric standard deviation σ, and number concentration N in nucleation (NuclM), Aitken (AitM), and accumulation mode (AccM) during spring (March, April, and May) and autumn (September, October, and November). Statistically significant (95% confidence level) trends are bolded, marked with an asterisk, and highlighted with border lines. Trends have been calculated using Sen-Theil estimator and complemented with bootstrap confidence intervals (see section 2.3.2).
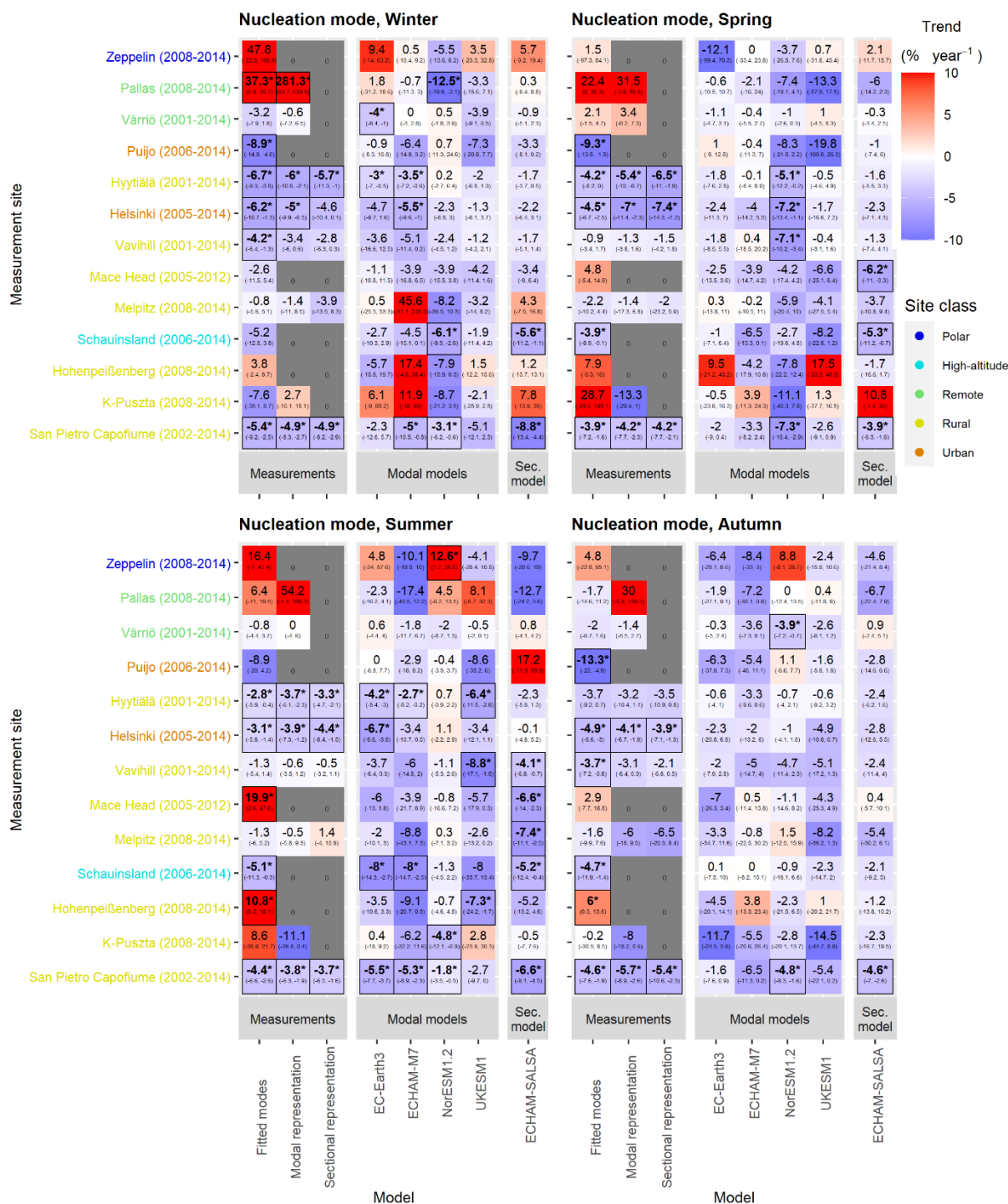
Figure S10 Seasonal trend estimates for nucleation mode number concentration for four seasons: winter (Jan, Feb, Dec), spring (Mar, Apr, May), summer (Jun, Jul, Aug), and autumn (Sep, Oct, Nov). Sites are ordered from most northerly to most southerly. The bolded number, asterisk, and line border around the estimate indicate that the trend is statistically significant (95% confidence level). Trends have been calculated using Sen-Theil estimator and complemented with bootstrap confidence intervals (see section 2.3.2).
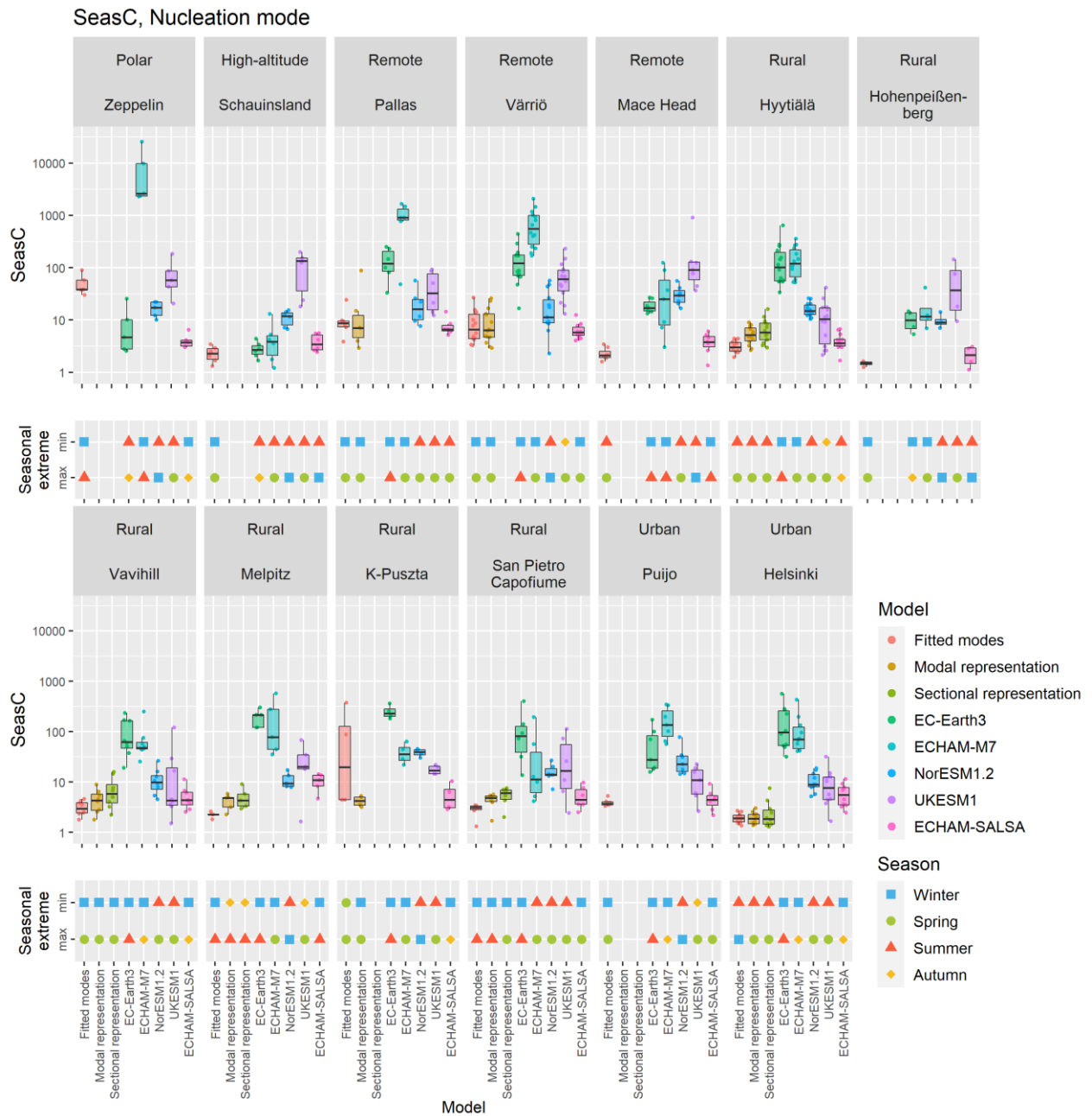
Figure S11 Maximum seasonal variation and seasonal extremes of nucleation mode particles for measurements and climate models. Upper panel: Ratio of maximum and minimum seasonal number concentration (SeasC) for measured and modeled nucleation mode. Points represent SeasC values for single years and box represents the quartiles (1st quartile, median, and 3rd quartile) of SeasC of certain measurement/model in certain site. Whiskers are 1.5*interquartile range. Lower panel: Seasons that most often have had minimum and maximum of number concentrations in measured and modeled nucleation mode.
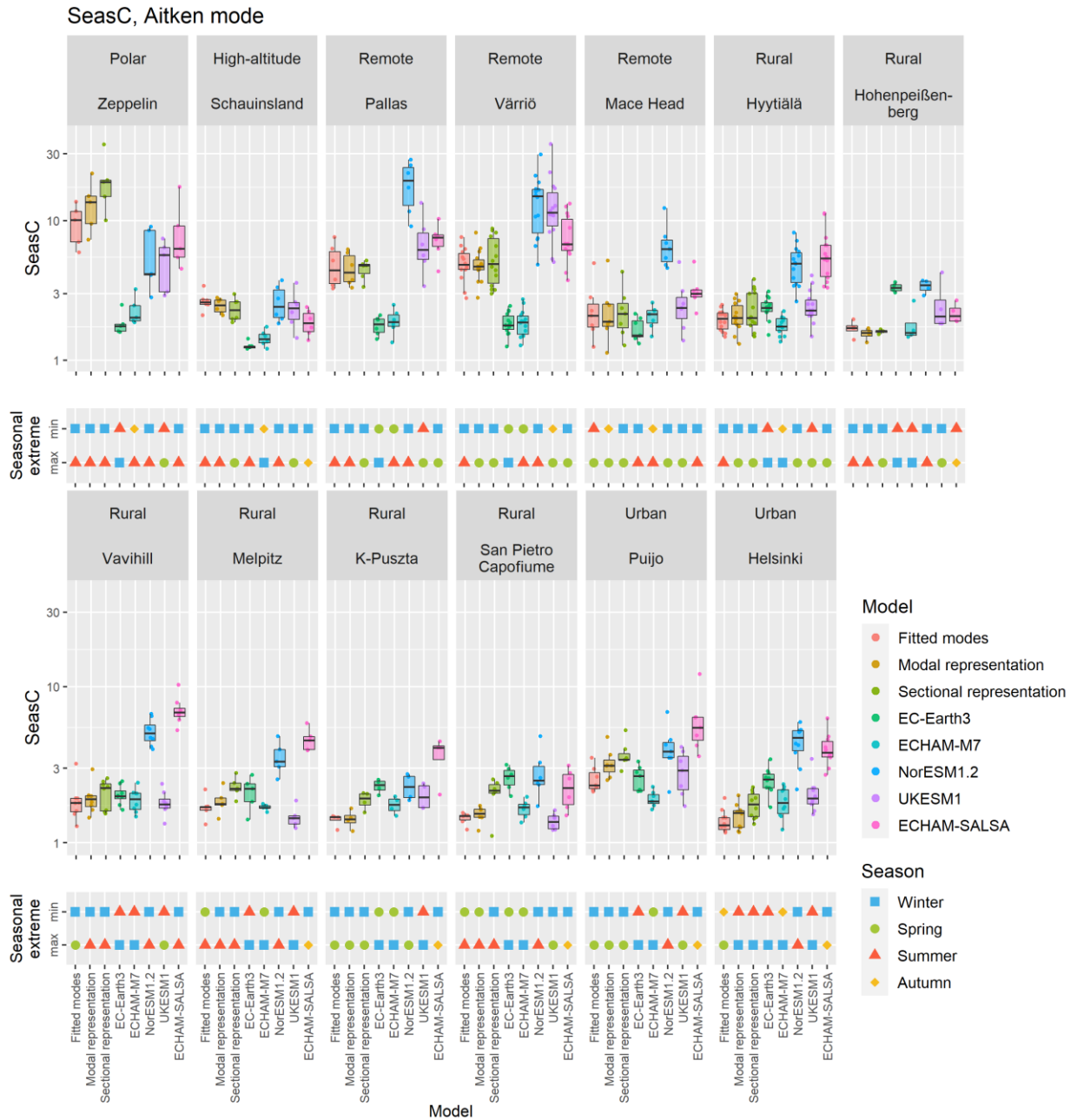
Figure S12. Maximum seasonal variation and seasonal extremes of Aitken mode particles for measurements and climate models. Upper panel: Ratio of maximum and minimum seasonal number concentration (SeasC) for measured and modelled Aitken mode. Points represent SeasC values for single years and box represents the quartiles (1st quartile, median, and 3rd quartile) of SeasC of certain measurement/model in a selected site. Whiskers are 1.5*interquartile range. Lower panel: Seasons that most often have had minimum and maximum number concentrations in measured and modeled Aitken mode.

Figure S13. Maximum seasonal variation and seasonal extremes of accumulation mode particles for measurements and climate models. Upper panel: Ratio of maximum and minimum seasonal number concentration (SeasC) for measured and modelled accumulation mode. Points represent SeasC values for single years and box represents the quartiles (1st quartile, median, and 3rd quartile) of SeasC of certain measurement/model in a selected site. Whiskers are 1.5*interquartile range. Lower panel: Seasons that most often have had minimum and maximum number concentrations in measured and modeled accumulation mode.
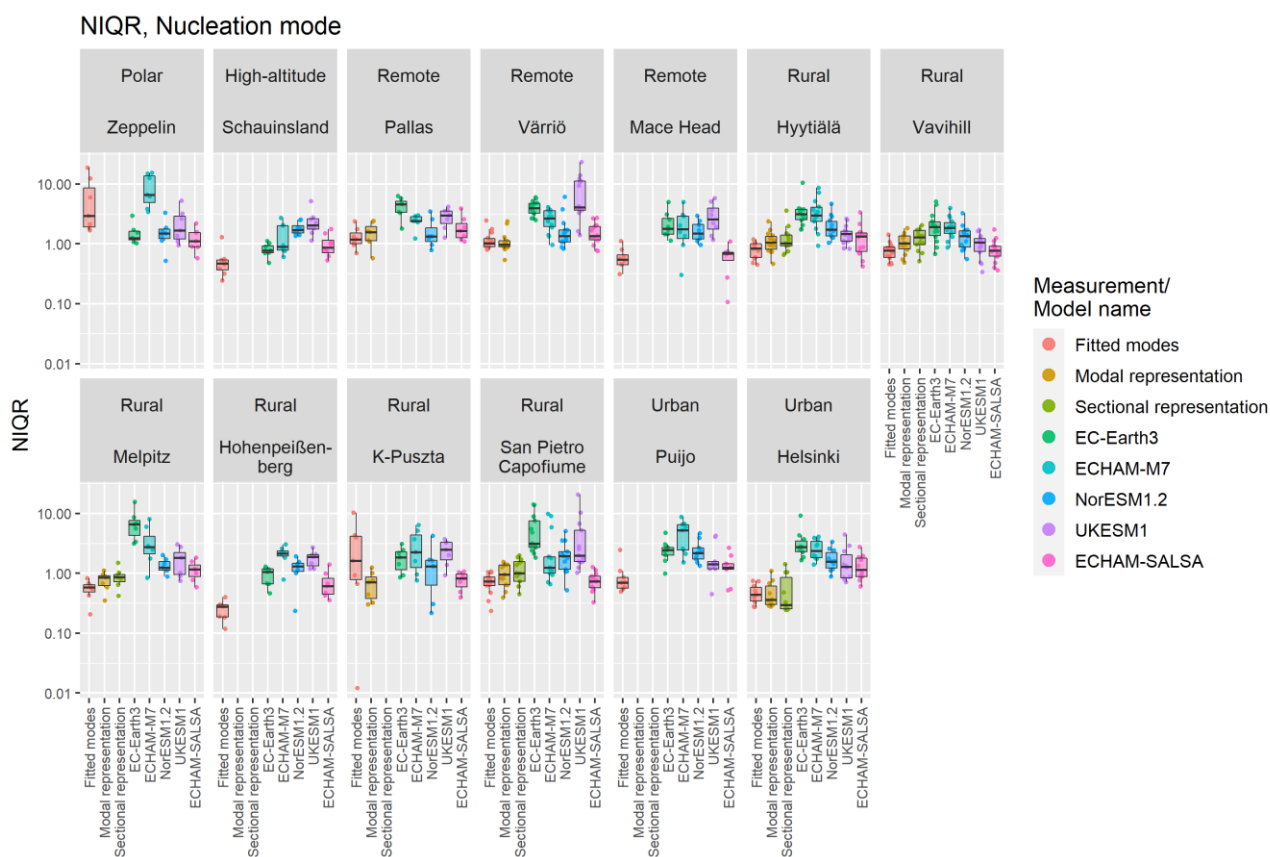
Figure S14 Average seasonal variation and seasonal extremes of nucleation mode particles for measurements and climate models. Normalized Interquartile Range (NIQR) for measured and modeled nucleation mode number concentration in different sites. Points represent NIQR values for single years and box represents the quartiles (1st quartile, median, and 3rd quartile) of NIQR of certain measurement/model in certain site. Whiskers are 1.5*interquartile range.
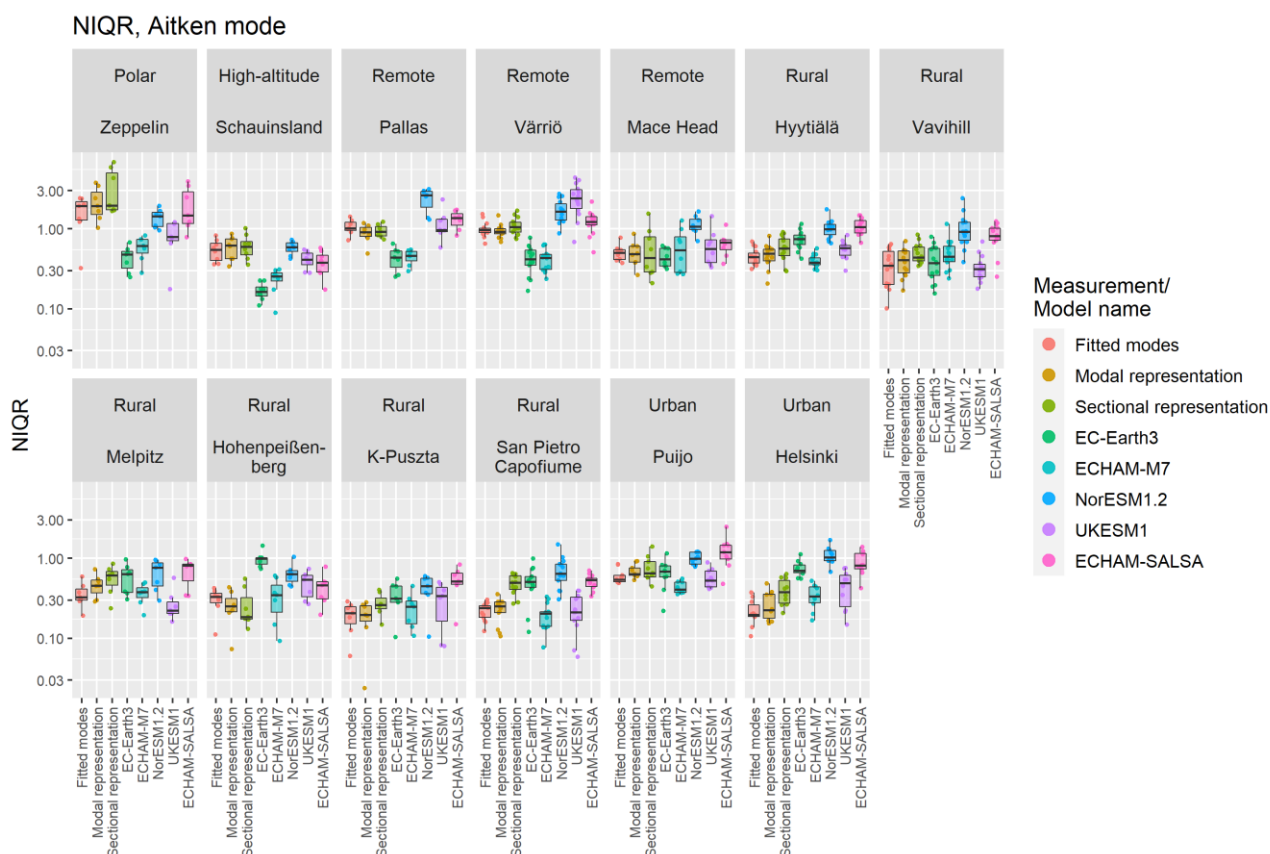
Figure S15 Average seasonal variation and seasonal extremes of Aitken mode particles for measurements and climate models. Normalized Interquartile Range (NIQR) for measured and modeled Aitken mode number concentration in different sites. Points represent NIQR values for single years and box represents the quartiles (1st quartile, median, and 3rd quartile) of NIQR of certain measurement/model in certain site. Whiskers are 1.5*interquartile range.
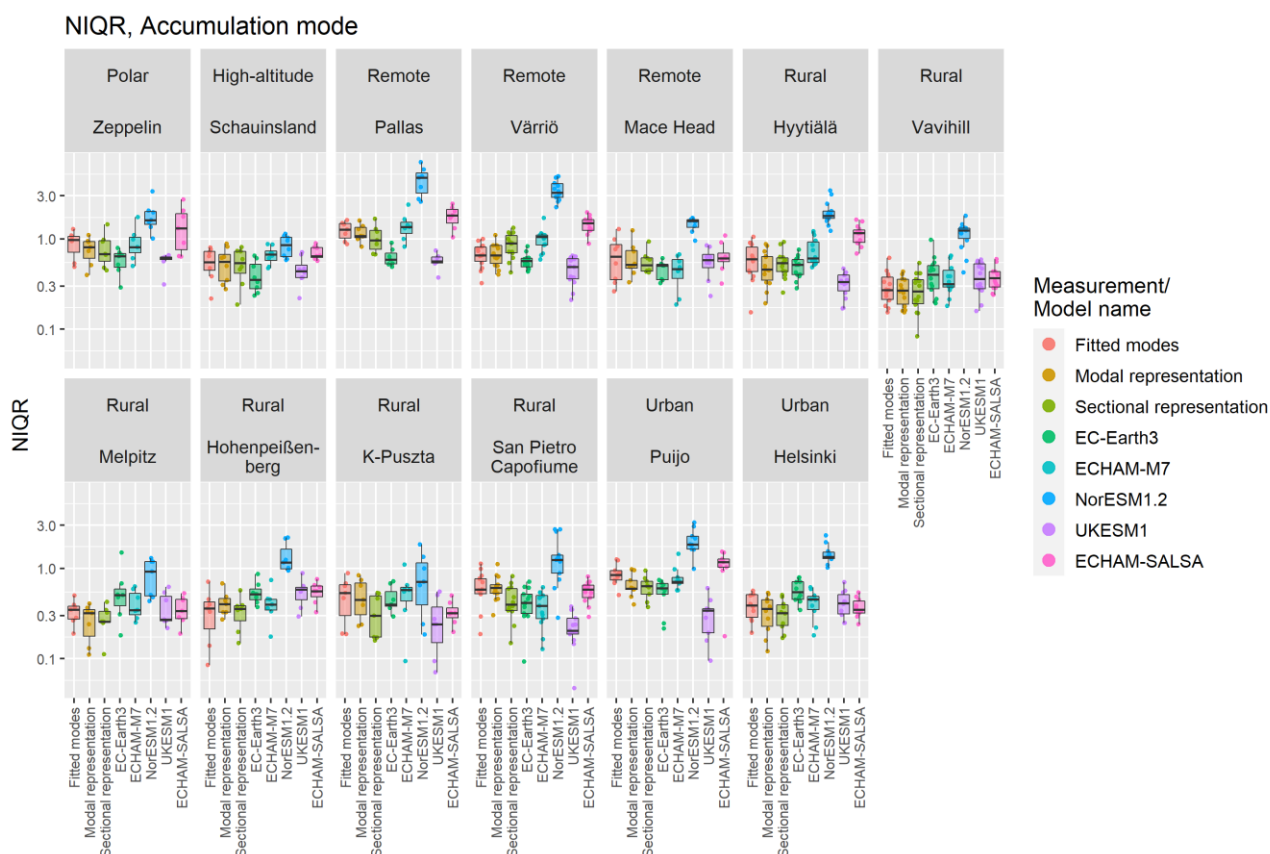
Figure S16 Average seasonal variation and seasonal extremes of accumulation mode particles for measurements and climate models. Normalized Interquartile Range (NIQR) for measured and modeled accumulation mode number concentration in different sites. Points represent NIQR values for single years and box represents the quartiles (1st quartile, median, and 3rd quartile) of NIQR of certain measurement/model in certain site. Whiskers are 1.5*interquartile range.
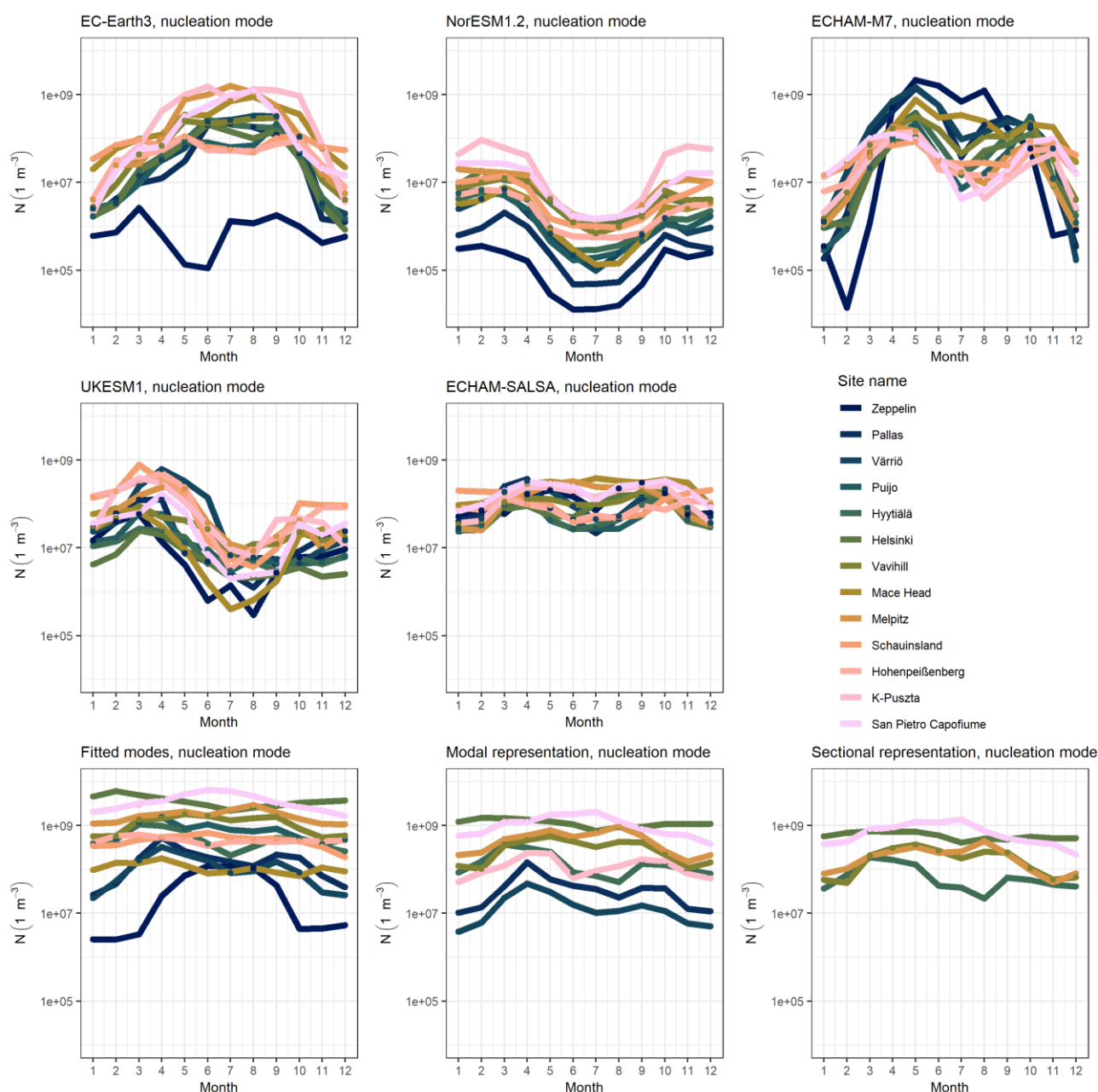
Figure S17 Seasonal cycle of nucleation mode number concentration in measurements and climate models for measurement sites. A subplot represents the seasonal cycle in one model or measurement. Coloured lines represent the median of the monthly means for Aitken mode number concentrations. Sites are ordered from most northerly to most southerly.

References

Rose, C., Collaud Coen, M., Andrews, E., Lin, Y., Bossert, I., Lund Myhre, C., Tuch, T., Wiedensohler, A., Fiebig, M., Aalto, P., Alastuey, A., Alonso-Blanco, E., Andrade, M., Artíñano, B., Arsov, T., Baltensperger, U., Bastian, S., Bath, O., Beukes, J. P., Brem, B. T., Bukowiecki, N., Casquero-Vera, J. A., Conil, S., Eleftheriadis, K., Favez, O., Flentje, H., Gini, M. I., Gómez-Moreno, F. J., Gysel-Beer, M., Hallar, A. G., Kalapov, I., Kalivitis, N., Kasper-Giebl, A., Keywood, M., Kim, J. E., Kim, S.-W., Kristensson, A., Kulmala, M., Lihavainen, H., Lin, N.-H., Lyamani, H., Marinoni, A., Martins Dos Santos, S., Mayol-Bracero, O. L., Meinhardt, F., Merkel, M., Metzger, J.-M., Mihalopoulos, N., Ondracek, J., Pandolfi, M., Pérez, N., Petäjä, T., Petit, J.-E., Picard, D., Pichon, J.-M., Pont, V., Putaud, J.-P., Reisen, F., Sellegri, K.,

Sharma, S., Schauer, G., Sheridan, P., Sherman, J. P., Schwerin, A., Sohmer, R., Sorribas, M., Sun, J., Tulet, P., Vakkari, V., van Zyl, P. G., Velarde, F., Villani, P., Vratolis, S., Wagner, Z., Wang, S.-H., Weinhold, K., Weller, R., Yela, M., Zdimal, V. and Laj, P.: Seasonality of the particle number concentration and size distribution: a global analysis retrieved from the network of Global Atmosphere Watch (GAW) near-surface observatories, Atmos. Chem. Phys., 21(22), 17185–17223, doi:10.5194/acp-21-17185-2021, 2021.